Laser-Induced Temperature Jump Measurements in the Kinetics of Association and Dissociation of the $N_2O_3 + M = NO_2 + NO + M$ System

B. Markwalder,† P. Gozel, and H. van den Bergh*

IGE-Pollution Atmosphérique et Sol and Laboratoire de Chimie Technique, Ecole Polytechnique Fédérale de Lausanne, CH-1015 Lausanne, Switzerland

Received: August 3, 1992; In Final Form: December 14, 1992

The kinetics of the $N_2O_3 + M = NO + NO_2 + M$ reaction has been studied over a wide range of pressure by a laser-induced temperature jump relaxation method. Equilibrium mixtures at 225 K containing nitrogen dioxide, dinitrogen trioxide, dinitrogen tetroxide, nitric oxide, a small quantity of SiF_4 as an IR absorber, and an excess of argon as a third-body gas collider are rapidly heated by a short pulse of CO_2 laser radiation. The induced temperature jump, between 0.5 and 3 K, displaces the equilibrium toward NO_2 and NO formation. The rate of relaxation to the new equilibrium concentrations at higher temperature is monitored by observing spectroscopically the time dependence of the N_2O_3 concentration in the UV. For small perturbations, simple mathematics relates the measured chemical relaxation time constant to the thermal rate constants of the $N_2O_3 + M = NO + NO_2 + M$ system. Experimental results, obtained in the 0.5–200 bar pressure range of argon corresponding to the third-order and falloff region of the reaction have been fitted by falloff curves established according to a method developed by Troe. The following high- and low-pressure limiting rate constants for the $NO + NO_2$ recombination at 227 K are extrapolated from the experimental data: $k_{rec,\infty} = (3.5 \pm 1.0) \times 10^{12}$ cm^3 mol^{-1} s^{-1} and $k_{rec,o}/[Ar] = (1.0 \pm 0.5) \times 10^{15}$ cm^3 mol^{-1} s^{-1}, respectively. These values lie within a factor of 2 of those that may be predicted using a simplified statistic adiabatic channel (SAC) model. The temperature dependence of the recombination rate constant, measured experimentally between 227 and 260 K, yields the following expressions for the high-pressure and the low-pressure limiting rate constants, respectively: $k_{rec,\infty}(T) = (1.6^{+1.6}_{-0.5}) \times 10^9 T^{(1.4\pm0.2)}$ cm^3 mol^{-1} s^{-1}, and $k_{rec,o}(T)/[Ar] = (1.0^{+1.0}_{-0.6}) \times 10^{33} T^{-(7.7\pm0.8)}$ cm^3 mol^{-1} s^{-1}.

Introduction

Thermal unimolecular gas-phase reactions, such as isomerization and bond dissociation, and the reverse recombination reactions are among the simplest chemical processes. The bond energy involved in these reactions may be as high as several hundred kJ/mol or more when a strong chemical bond is broken. At the other end of the energy scale, however, dissociation energies of only a few kJ/mol may be involved when weak van der Waals adducts or hydrogen-bonded molecules are dissociated. The kinetics of thermal recombination reaction involving free radicals, and the reverse dissociation reactions has been quite well studied from both the theoretical and experimental point of view for several decades.[1-4] Experimental results, obtained at high temperatures when breaking bonds, or at low temperatures in radical association processes, can generally be well fitted by the RRKM theory and its extensions.[4] These theories are based on a rapid randomization of the internal energy among the available states before the local energy is sufficient to break, in most cases, the weakest chemical bond within the molecule.

On the other hand, some disagreement between theory and experiment has been observed in weakly bound systems which involve hydrogen bonds or van der Waals forces. For example, in spectroscopic studies, sharp lines may be found in overtones where the upper vibrational state lies well above the dissociation energy of the weakest bond.[5] This suggests that the reaction rate might start to compete with intramolecular energy transfer, so that classical statistical theories may no longer apply. To search for the limits of applicability of statistical theories, it appears of interest to measure the kinetics of systems with intermediate and weak bond energies. Hence, we have developed a laser T-jump method which is particularly suitable to investigate such reactions with small enthalpy change and small activation energies. To test this method, we have previously investigated the $N_2O_4 + M = 2NO_2 + M$ chemical equilibrium[6] in the falloff region between 0.3 and 200 bar. With a N–N bond energy in N_2O_4 of about 56.4 kJ/mol, this system has been widely studied to date.[7-10] Reaction rate constants, determined experimentally by flash photolysis,[9] in shock wave tubes,[8] and by laser-induced chemical relaxation,[7] are in good agreement with one another and with those extrapolated from theoretical models.

The present paper gives the results on a system with still a lower bond dissociation energy, i.e., $N_2O_3 + M = NO_2 + NO + M$, in which the N–N bond energy in N_2O_3 is close to 41.0 kJ/mol.[11-13] The N_2O_3 vibrational frequencies necessary for the calculations are well-known from the literature;[14-15] they range from $\nu = 70$ cm^{-1} for the torsional mode around the N–N bond to $\nu = 1832$ cm^{-1} for the stretching mode of the N–O bond. The $N_2O_3 + M = NO_2 + NO + M$ reaction has been studied recently by Smith et al.[16,17] They used a chemical relaxation method, in which a small fraction of N_2O_3 in equilibrium with NO and NO_2 is removed by flash photolysis; the rate of relaxation back to the new equilibrium is then observed by monitoring the time dependence of the N_2O_3 concentration in the IR. Experimental results cover a limited range of pressures from about 0.2 to 10 atm, which corresponds to the third-order region and the beginning of the falloff range. In these conditions, extrapolation of the experimental data to yield the recombination rate constant in the high-pressure limit may lead to very large uncertainties.

The present work presents measurements for pressures up to 200 bar of argon. A chemical relaxation method is applied in which the chemical equilibrium is perturbed by a small laser-induced temperature jump of less than 3 K, and subsequent monitoring of the N_2O_3 concentration is done in the UV. This technique has already been established in a study of the $N_2O_4 = 2\ NO_2$ system.[6-10]

* To whom correspondence should be addressed.
† Laboratoire de Chimie Technique.

0022-3654/93/2097-5260$04.00/0

Experimental Section

The experiments were carried out with an experimental setup similar to that used in our previous work, and details can be found in the literature.[6,18,19] Briefly, a thermostated cylindrical cell is placed between two quartz plates which are oriented at 45° in respect to the cell's main axis. The Reststrahlung reflection of the IR beam on the quartz plates[20,21] and the transmission of the continuous-wave (cw) UV-analyzing beam through these plates allow for coaxial passing of the two beams along the axis of the reaction cell. The cell is closed with two 12-mm-thick BaF_2 windows (Harshaw) which have suitable transmission at both the UV and IR wavelengths. Omniseal O-rings (Johannsen AG) are used at pressures up to 200 bar and temperatures down to 220 K. The pulsed TEA CO_2 laser (TE 821-HP, Lumonics) is tuned to 9.694 μm (9P36) in order to excite SiF_4, which is the IR sensitizer used throughout this work. At this wavelength, pulses of about 2.5 J in a spike of 120 ns and a tail extending over less than 0.5 μs and containing less than 25% of the energy are obtained. The cw analyzing beam from a 200-W high-pressure mercury–xenon lamp is collimated and then filtered by a reflection filter (R250, Oriel), λ_{max} = 253 nm, T_{max} = 74%, fwhm = 43 nm, in order to monitor N_2O_3 by its absorption in the UV. An electromechanical shutter (Uniblitz), placed in the cw beam, is opened a few ms before a T-jump experiment and closed rapidly afterward, in order to avoid significant NO_2 photolysis.[22] The temporal variation of the transmitted light at 253 nm, corresponding essentially to the variation in N_2O_3 concentration following the laser induced temperature jump, is detected by a photomultiplier tube (1P28A, RCA) and recorded by a signal averaging digital oscilloscope (LeCroy 9400). SiF_4 is degassed at 77 K by several freeze–pump–thaw cycles prior to use. NO_2 (99.6%, Matheson) is dried over molecular sieve and reacted overnight with an excess of O_2 to oxidize possible NO impurities to NO_2. The O_2 excess is removed by pumping at 193 K and the NO_2/N_2O_4 mixture is finally outgassed at 77 K and stored in the dark at room temperature. NO (99%, Linde) is purified by pumping through a U-tube cooled at 193 K to trap any NO_2/N_2O_4 impurities; this process is repeated five times before further purification is carried out by three consecutive freeze–pump–thaw cycles at 77 K. The purified NO is finally stored in the dark at room temperature. Argon (99.998%, Carbagas) is used without further purification.

Results

Chemical Relaxation. Equilibrium mixtures of NO_2 and NO contain various concentrations of NO, NO_2, N_2O_3, and N_2O_4 depending on temperature and the ratio of the NO and NO_2 concentrations. For simplification purposes, $[NO]^*$ is introduced in a large excess in respect to $[NO_2]^*$, where $[NO]^* = [NO] + [N_2O_3]$ and $[NO_2]^* = [NO_2] + [N_2O_3] + 2[N_2O_4]$.

The thermodynamics of the dinitrogen trioxide dissociation has been the subject of numerous studies during the past years.[11-13] For the reaction

$$N_2O_3 + M \underset{k_{rec}}{\overset{k_{diss}}{\rightleftarrows}} NO_2 + NO + M \qquad \Delta H_r^\circ = 41.0 \text{ kJ/mol}^{11-13} \tag{1}$$

an expression for the equilibrium constant

$$K_1 = [NO_2][NO]/[N_2O_3] \tag{2}$$

as a function of the temperature may be deduced from the work of Chao,[12] and written as

$$K_1(T) = 2.98 \times 10^5 T^{-1} \exp\{-(4.88 \times 10^3)/T\} \tag{3}$$

with $K_1(T)$ expressed in mol/cm³.

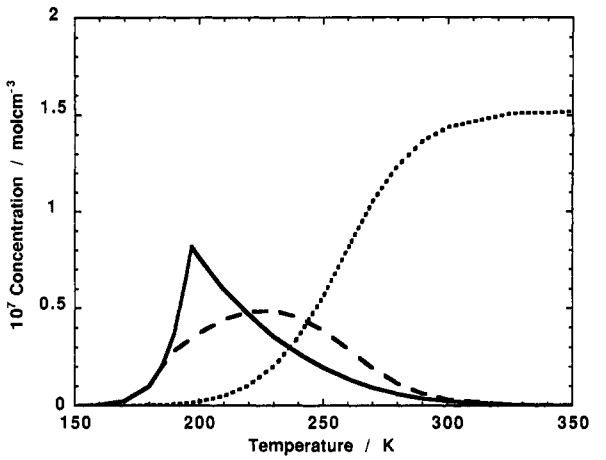

Figure 1. Concentrations of NO_2 (···), N_2O_3 (—), and N_2O_4 (– –) versus temperature in equilibrium mixtures containing 26.6 mbar of $[NO]^* = [NO] + [N_2O_3]$ and 2.86 mbar of $[NO_2]^* = [NO_2] + [N_2O_3] + 2[N_2O_4]$.

Similarly, for the dinitrogen tetroxide equilibrium

$$N_2O_4 + M \rightleftarrows NO_2 + NO_2 + M \qquad \Delta H_r^\circ = 56.4 \text{ kJ/mol}^{23} \tag{4}$$

the temperature dependence of the equilibrium constant is given by

$$K_4(T) = 1.27 \times 10^7 T^{-1} \exp\{-(6.79 \times 10^3)/T\} \tag{5}$$

in units of mol/cm³, based on the work of Vosper.[23]

Using the expressions 3 and 5 and with suitable mass balance relations, the temperature dependence of each species in the reaction mixture containing 2.86 mbar (1.53×10^{-7} mol/cm³) NO_2^* and 26.6 mbar (1.42×10^{-6} mol/cm³) NO^* can be found in Figure 1. It can be seen that $[N_2O_3]$ reaches a maximum at about 197 K; at lower temperatures, N_2O_3 solidifies, and the partial pressure of N_2O_3 over the solid decreases rapidly with decreasing temperature.[24] On the other hand, the decrease of $[N_2O_3]$ above 197 K is due to dissociation into $NO_2 + NO$ according to eq 1. Figure 1 also shows that the variation of the N_2O_3 concentration in function of the temperature, i.e., $|[N_2O_3]/\Delta T|$ is maximum just above 197 K and decreases with increasing temperature. To observe the highest sensitivity, it is therefore preferable to work at temperatures as low as possible, above the limits where deposition of solid N_2O_3 on the cell windows becomes significant. The experiments were carried out at initial temperatures near 225 K. At these temperatures, the reaction cell could still be efficiently cooled by circulating thermostated ethanol, and the O-rings used still give a good vacuum. Moreover, as illustrated in Figure 1, possible interference in the optical signal caused by the variation in N_2O_4 concentration is minimized around 225 K (N_2O_4 also absorbs around 253 nm where N_2O_3 is monitored).

Figure 2 shows a typical oscilloscope trace when the N_2O_3 concentration is monitored around 253 nm following a laser-induced temperature jump of 0.7 K. The initial temperature is 226.3 K, and the reaction mixture contains 100 μbar (5.34×10^{-9} mol/cm³) SiF_4, 2.86 mbar (1.53×10^{-7} mol/cm³) NO_2^*, 26.6 mbar (1.42×10^{-6} mol/cm³) NO^* and 0.5 bar (2.67×10^{-5} mol/cm³) argon. The trace is the result of signal averaging over 100 laser shots. The decrease in N_2O_3 over a period of 20 μs illustrates the chemical relaxation of the gas mixture to the new equilibrium concentrations at the higher temperature, i.e. T_f = 227 K, following the temperature jump.

To establish the mathematical expressions relating the observed relaxation time to the kinetics of dissociation of N_2O_3, the following hypothesis are made:

(1) Since an excess of NO is present in the reaction mixture, [NO] is much greater than the variation of N_2O_3 concentration

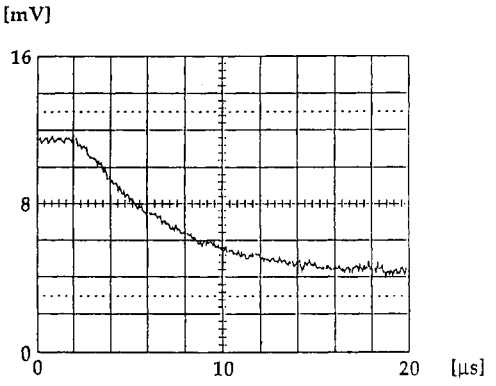

Figure 2. Oscilloscope trace corresponding to a 0.7 K laser induced temperature jump in a mixture containing 100 μbar of SiF_4, 2.86 mb $[NO_2]^*$, 26.6 mbar of $[NO]^*$, and 0.5 bar of argon. The trace is the result of signal averaging over 100 laser shots.

during the perturbation, and therefore [NO] is assumed to be constant during the experiment, i.e., $[NO] \approx [NO]^*$.

(2) Besides N_2O_3, N_2O_4 is formed in the reaction mixture, i.e. equilibrium (4;–4); this will partially dissociate to NO_2 following the T-jump. However, from previous kinetic studies, as the relaxation kinetics of the $N_2O_3 = NO_2 + NO$ equilibrium[17] is at least an order of magnitude faster than that of the $N_2O_4 = 2\,NO_2$ system,[6,9] the contribution of the dissociation of N_2O_4 to yield NO_2 can essentially be neglected on the time scale of the N_2O_3 observation. In any case, as pointed out above, the change in N_2O_4 concentration is much smaller than the one of N_2O_3 around 225 K, so that the optical perturbation due to reactions (4;–4) would be negligible anyway.

(3) Very small perturbations, i.e., $\Delta[N_2O_3] \ll [N_2O_3]$, are induced; under these conditions, linearization of the perturbation equations is therefore possible.

With these hypothesis, the relaxation time τ of the chemical system (1;–1) can be related to the recombination rate constant k_{rec} by a mathematical development similar to the one published in detail elsewhere:[18,19]

$$k_{rec} = \frac{1/\tau}{[NO]^* + K_{1,f}} \qquad (6)$$

$[NO]^*$ is the excess concentration of NO introduced in the reaction mixture, and $K_{1,f}$ is the equilibrium constant of (1;–1) at the final temperature T_f calculated by the following way:

(a) $[N_2O_3]_i$ and $[NO_2]_i$, the initial concentrations of respectively N_2O_3 and NO_2 present in the reaction mixture at T_i, are determined from the knowledge of the partial pressures of NO and N_2O_4/NO_2 introduced in the reaction cell, and the known thermodynamics and suitable mass balance relations.

(b) The change in concentration of N_2O_3, $\Delta[N_2O_3]_{i,f}$, corresponding to the equilibrium N_2O_3 concentration change between T_i and T_f, is determined from the trace in Figure 2:

$$\Delta[N_2O_3]_{i,f} = \frac{\log\{I/(I + \Delta I_{max})\}}{\epsilon_{eff} d} \qquad (7)$$

where I is the signal intensity prior to the temperature jump at T_i, and ΔI_{max} the difference of beam intensity before and right after the concentration jump. The cell length is d, and ϵ_{eff} is the effective decadic molar extinction coefficient of N_2O_3 around 253 nm at the applied conditions; it is measured to be $\epsilon_{eff} = 1560 \pm 70$ L mol^{-1} cm^{-1} and is found to be essentially independent of temperature and pressure in the limits 220–265 K and 0.5–200 bar of argon.

(c) the N_2O_3 concentration $[N_2O_3]_f$ at the final temperature T_f can then be calculated by

$$[N_2O_3]_f = [N_2O_3]_i + \Delta[N_2O_3]_{i,f} \qquad (8)$$

Assuming again a slow chemical relaxation kinetics for the N_2O_4/NO_2 system, the contribution of the N_2O_4 dissociation to the change of concentration of NO_2 may be neglected, and therefore $\Delta[NO_2]_{i,f} = -\Delta[N_2O_3]_{i,f}$. The final concentration of NO_2 at T_f is given by $[NO_2]_f = [NO_2]_i + \Delta[NO_2]_{i,f}$, and K_{1f}, the equilibrium constant at T_f is finally calculated by introducing in eq 2 the final concentrations of NO_2 and N_2O_3 following the temperature jump, and $[NO]^*$, the excess concentration of NO. The value of T_f and therefore the size of the temperature jump, $\Delta T = T_f - T_i$, may be determined with eq 3.

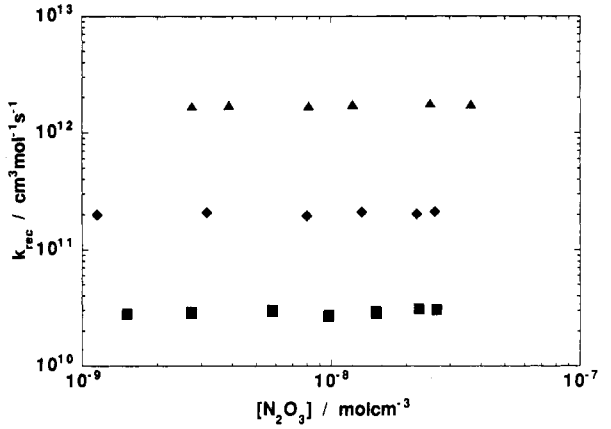

Figure 3. Recombination rate constant k_{rec} of $NO + NO_2 + Ar \rightarrow N_2O_3 + Ar$ versus the N_2O_3 concentration, at three different argon pressures, i.e., p = 0.5, 5.0, and 200 bar. The laser induced temperature jump is about 2 K, and the final temperature 227 K.

Pressure Dependence of k_{rec}

For the chemical equilibrium $N_2O_3 + M = NO_2 + NO + M$, the pressure dependence of k_{rec}, the recombination rate constant, has been measured at 227 K. In the domain of pressures studied, i.e., 0.5–200 bar added argon, the kinetics is strongly influenced by collisional activation/deactivation processes. For the interpretation of the data, it is preferable that these processes are dominated by a single bath gas which has a unique collisional activation/deactivation efficiency β_c.[1-4] Therefore, for each pressure of added argon, experiments with various concentrations of N_2O_3 were carried out at 227 K. Figure 3 shows the results for three argon pressures, i.e., 0.5, 5.0, and 200 bar. It can be seen that k_{rec} is weakly dependent on the N_2O_3 concentration at these argon pressures. At the higher pressure in particular, where argon is in large excess, k_{rec} essentially does not depend on $[N_2O_3]$ at all. In any case, the extrapolation to $[N_2O_3] = 0$, where activation/deactivation processes are entirely dominated by argon, appears straightforward. In this aspect, the behavior of the $N_2O_3/NO_2 + NO$ system contrasts with that of the $N_2O_4 = 2NO_2$ system. In the latter, "step-shaped" curves have been observed at low bath gas pressures.[6] Such effects were attributed to direct V–V energy transfer between SiF_4^*, the excited IR-sensitizer, and N_2O_4, followed by fast $N_2O_4^* \rightarrow 2NO_2$, leading to an uncomplete thermal relaxation prior to reaction.

The values of k_{rec} in Ar and the complete falloff curve obtained from the experimental points are represented in Figure 4, and the measured data points are also listed in Table I. The temperature is 227 K. Each point of Figure 4 represents the extrapolated value to $[N_2O_3] = 0$ of $k_{rec} = f([N_2O_3])$ curves as illustrated in Figure 3. Signal averaging over hundreds of laser shots allows the method to be applied at total pressures as low as 0.5 bar. In this case, reaction mixtures still contain a 20-fold excess of argon as third-body gas collider in respect to $[NO]^*$, which is itself about 10 times more abundant that $[NO_2]^*$. The highest pressure at which experiments were carried out, i.e., 200 bar, is limited by the elastic limit of the 34-mm diameter, 12-mm-thick BaF_2 windows used in our stainless steel cell.

To extrapolate to the high- and low-pressure limiting values of k_{rec} in Ar, the experimental points have been fitted by a falloff

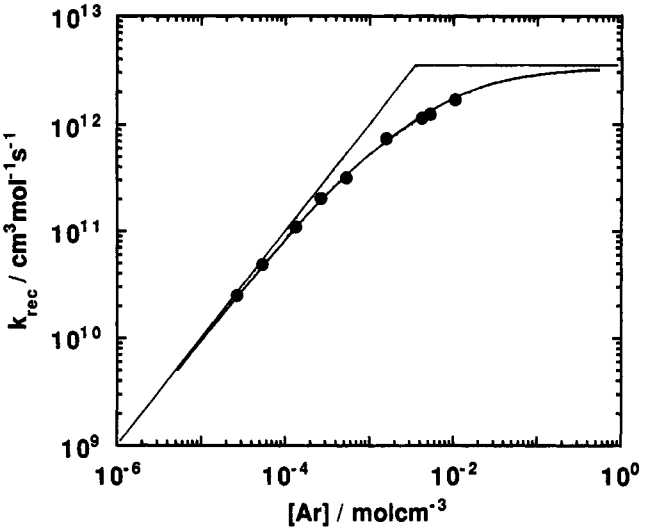

Figure 4. Falloff curve of the reaction $NO + NO_2 + Ar \rightarrow N_2O_3 + Ar$ at 227 K. The best fit through the experimental data leads to $k_{rec,\infty} = (3.5 \pm 1.0) \times 10^{12}$ cm^3 mol^{-1} s^{-1} and $k_{rec,o}/[Ar] = (1.0 \pm 0.5) \times 10^{15}$ cm^3 mol^{-1} s^{-1}.

curve, as proposed by Troe et al.[3,25,26]

$$\log\left(\frac{k_{rec}}{k_{rec,\infty}}\right) = \log\left(\frac{k_{rec,o}/k_{rec,\infty}}{1 + (k_{rec,o}/k_{rec,\infty})}\right) + \frac{\log F_{cent}}{1 + \left(\frac{\log(k_{rec,o}/k_{rec,\infty})}{N}\right)^2} \quad (9)$$

The shape of the curve is determined by the parameters F_{cent} and N. Accordingly to refs 3, 25, and 26, $F_{cent} = 0.60$ and $N = 1.03$ for the $N_2O_3 + Ar = NO_2 + NO + Ar$ reaction. $k_{rec,\infty}$ and $k_{rec,o}$, the recombination rate constants in the high and low-pressure limits, respectively, are adjusted in a trial-and-error fashion in order to obtain the best fit through the experimental data. This leads to $k_{rec,\infty} = (3.5 \pm 1.0) \times 10^{12}$ cm^3 mol^{-1} s^{-1} and $k_{rec,o}/[Ar] = (1.0 \pm 0.5) \times 10^{15}$ cm^3 mol^{-1} s^{-1}. The error limits include the experimental uncertainties in the extrapolation to $[N_2O_3] = 0$ of the k_{rec} versus $[N_2O_3]$ curves. These experimental determinations of $k_{rec,\infty}$ and $k_{rec,o}$ are compared to values calculated by simplified versions of the RRKM theory and its extensions, which are particularly suited for association/dissociation reactions. The details of the calculations are given below:

$k_{rec,o}$: In the low-pressure range, where intermolecular energy transfer is rate limiting, the rate constant $k_{rec,o}$ is estimated using a factorized analytical expression, as described in refs 1–3:

$$\frac{k_{rec,o}}{[M]} = \frac{1}{K_1(T)}\beta_c(M)Z_{LJ}\frac{\rho_{vib,h}(E_0)kT}{Q_{vib}} \times \exp\left(\frac{E_0}{kT}\right)F_{anh}F_E F_{rot}F_{rot\ int} \quad (10)$$

Each term of eq 10 is evaluated for the $N_2O_3 + M = NO_2 + NO + M$ reaction at 227 K, with M = Ar. Only the results are given here; the reader is referred to refs 1–3 for the details of the calculations:

$K_1(T)$: equilibrium constant of (1;–1) at 227 K; $K_1(T) = 6.1 \times 10^{-7}$ mol/cm^3.

$\beta_c(M)$: collisional efficiency of M = Ar as a third-body collider; $\beta_c(Ar) = 0.30$.[27,28]

K_{LJ}: the expression of Z_{LJ}, the Lennard-Jones collisional frequency, is given in ref[3] for N_2O_3 in argon, $Z_{LJ} = 5.4 \times 10^{13}$ cm^3 mol^{-1} s^{-1}.

Q_{vib}: the vibrational function of partition, calculated with the N_2O_3 fundamental modes of vibration from the literature,[14,15] has for value $Q_{vib} = 5.4$.

TABLE I: Experimental Recombination Rate Constants k_{rec} versus Argon Pressure for the Reaction $NO + NO_2 + Ar \rightarrow N_2O_3 + Ar$ at 227 and 260 K

p(Ar)/bar	k_{rec}/cm^3 mol^{-1} s^{-1}	p(Ar)/bar	k_{rec}/cm^3 mol^{-1} s^{-1}
	$T = 227$ K		
0.5	2.5×10^{10}	30	7.5×10^{11}
1.0	4.9×10^{10}	80	1.2×10^{12}
2.5	1.1×10^{11}	100	1.3×10^{12}
5.0	2.1×10^{11}	200	1.7×10^{12}
10	3.2×10^{11}		
	$T = 260$ K		
0.5	6.50×10^{9}	10	1.11×10^{11}
1.0	1.35×10^{10}	50	4.78×10^{11}
5.0	6.05×10^{10}	200	1.05×10^{12}

$\rho_{vib,h}(E_0)$: the density of harmonic states at the dissociation threshold E_0 is estimated by a simplified model proposed by Whitten and Rabinovitch;[29] for $E_0 = 39.5$ kJ/mol,[11] one obtains $\sigma_{vib,h}(E_0) = 1.9$ mol/J.

The four correcting factors F_{anh}, F_E, F_{rot}, and $F_{rot\ int}$ may be estimated using the relations given by Troe.[1-3] They have for values the following: the anharmonicity correction: $F_{anh} = 1.38$; the correction due to the energy dependence of the density of states above the reaction threshold: $F_E = 1.24$; the correction due to the external rotation, with the approximation of a Morse type potential surface: $F_{rot} = 5.83$; the correction due to the internal rotation, with an energy barrier to rotation $V_o = 4.2$ kJ/mol:[14] $F_{rot\ int} = 3.5$.

Introducing the above estimations in eq 10, one obtains $k_{rec,o}/[Ar] = (5.0 \pm 0.5) \times 10^{14}$ cm^3 mol^{-1} s^{-1}.

$k_{rec,\infty}$: The intramolecular rearrangement of the energy in the activated complex constitutes the rate-determining step in the unimolecular dissociation of N_2O_3 in the high-pressure limit. According to the statistical adiabatic channel model (SAC) model, a simplified expression for $k_{rec,\infty}$ has been proposed by Quack and Troe:[4,30,31]

$$k_{rec,\infty} = \frac{kT}{h}\left(\frac{h^2}{2\pi\mu kT}\right)^{3/2}\frac{Q_{el}(N_2O_3)}{Q_{el}(NO_2)Q_{el}(NO)} \times \frac{Q^*_{cent}F^*_{AM}\frac{1}{\sigma^*}\Pi^b Q^*_m}{Q_{rot}(NO_2)Q_{rot}(NO)}\exp\left[-\frac{\Delta E_{o,z}}{kT}\right] \quad (11)$$

where h is the constant of Planck, μ is the reduced mass of the system: $\mu = 18.2$ g/mol, $Q_{el}(i)$ are the classical electronic partition functions; $Q_{el}(N_2O_3) = 1$, $Q_{el}(NO_2) = 2$, and $Q_{el}(NO) = 2.9$. $Q_{rot}(l)$ are the classical rotational partition functions; $Q_{rot}(NO_2) = 1460$, and $Q_{rot}(NO) = 92$. $\Delta E_{o,z}$ is the threshold energy for recombination on the lowest energy channel; $\Delta E_{o,z} = 90$ J/mol. The terms with an asterisk correspond to the activated complex and are functions of α, the looseness parameter of the angular part of the potential, and β, the Morse parameter of the radial part of the reaction coordinate. β can easily be calculated with the knowledge of the force constant of the breaking bond[4] and has for value $\beta = 1.11$ Å^{-1}. The looseness parameter, however, is more complicated to evaluate, and a standard value of $\alpha = 1$ Å^{-1} has been suggested.[30,31] According to the SAC model, it has been shown that $k_{rec,\infty}$ depends mostly on the α/β ratio, rather than on an absolute value of α.[4] α/β ratios have been tabulated for 26 reactions;[32] for the N_2O_3 dissociation, no value is available, but $\alpha/\beta = 0.56$ has been determined experimentally[6] for the dissociation of N_2O_4, a molecule somewhat similar to N_2O_3. $\Pi^b Q_m^*$, the pseudopartition function of the activated complex, may be evaluated according to the correlation diagram described in the Appendix: it is found $\Pi^b Q_m^* = 3.06 \times 10^3$. By a procedure given by Quack,[30,31] one calculates $Q^*_{cent} = 1.28 \times 10^4$, $F^*_{AM} = 3.20$, and $\sigma^* = 3.92$ for the activated complex; this leads to $k_{rec,\infty} = 2.3 \times 10^{12\pm0.5}$ cm^3 mol^{-1} s^{-1}.

Table II gives a summary of the calculated recombination rate constants in the high- and low-pressure limits, in comparison

TABLE II: Theoretical and Experimental Recombination Rate Constants for the Reaction NO + NO_2 + Ar → N_2O_3 + Ar at 227 K in the Low- and High-Pressure Domain

low pressure		high pressure	
$k_{rec,0}/[Ar]/cm^3\ mol^{-1}\ s^{-1}$		$k_{rec,\infty}/cm^3\ mol^{-1}\ s^{-1}$	
experimental	calculated	experimental	calculated
$(1.0 \pm 0.5) \times 10^{15}$	$(5.0 \pm 0.5) \times 10^{14}$ $\beta_c = 0.30$	$(3.5 \pm 1.0) \times 10^{12}$ $\alpha/\beta = (0.59 \pm 0.03)^a$	$2.3 \times 10^{(12\pm0.5)}$ $\alpha/\beta = 0.56^b$

[a] This work. [b] Reference 6.

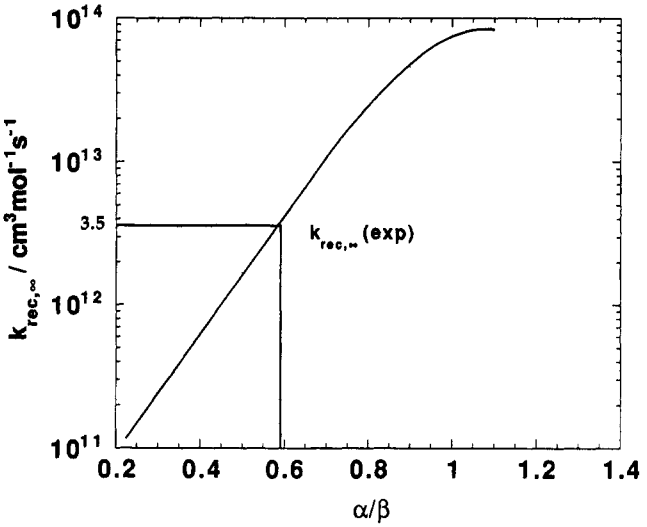

Figure 5. Recombination rate constant $k_{rec,\infty}$, calculated according to the SAC model, of the NO + NO_2 + Ar → N_2O_3 + Ar reaction in the high-pressure limit. $k_{rec,\infty}$ is shown versus the α/β ratio. The experimental value $k_{rec,\infty} = (3.5 \pm 1.0) \times 10^{12}$ cm^3 mol^{-1} s^{-1} leads to $\alpha/\beta = (0.59 \pm 0.03)$.

with those extrapolated from the experimental data. For the high-pressure limit, the theoretical calculations according to the SAC model lead to an underestimation of $k_{rec,\infty}$ by about 30%. This rather good agreement may in part be due to the wide range of pressures where experiments were carried out in order to cover a large part of the falloff region, thus reducing the uncertainties in the extrapolation of the experimental data. The main source of error in the calculations probably comes from the α/β ratio. With the exception of a few systems where ab initio calculations have been made,[33,34] α/β ratios are determined experimentally from a plot of $k_{rec,\infty}$ versus the α/β ratio, as represented in Figure 5 for the N_2O_3 dissociation. In this case, it is deduced $\alpha/\beta = (0.59 \pm 0.03)$, corresponding to $k_{rec,\infty} = (3.5 \pm 1.0) \times 10^{12}$ cm^3 mol^{-1} s^{-1}, our extrapolated experimental value of the recombination rate constant. This value of α/β corresponds to an intermediate between a typically loose ($\alpha/\beta > 1.0$) and a rigid ($\alpha/\beta \to 0$) activated complex. In the case of the low-pressure limit, the calculated value of the recombination constant is a factor of 2 lower than the experimental value. Extrapolation of the data to the low-pressure limit probably leads to small uncertainties as can be seen from Figure 3. However, large uncertainties in the low vibrational frequencies, and in the calculation of the rotational correcting factor F_{rot}, which depends on the type of potential surface used, may lead to the low calculated value of $k_{rec,0}$. Furthermore, it should be realized that in the SAC model, the potential surface is oversimplified which, among others, may lead to errors in the values predicted by the statistical theory.

Temperature Dependence of k_{rec}

A second falloff curve $k_{rec} = f([Ar])$ has been established at 260 K in order to determine the temperature dependence of the recombination rate constant in the low- and high-pressure limits. The best fit through the experimental data, as shown in Figure 6, lead to $k_{rec,0}/[Ar] = (3.3 \pm 1.6) \times 10^{14}$ cm^{-3} mol^{-1} s^{-1} and $k_{rec,\infty} = (4.3 \pm 1.2) \times 10^{12}$ cm^3 mol^{-1} s^{-1}. By a regression, one obtains in the domain 225–260 K: $k_{rec,0}(T)/[Ar] = (1.0^{+1.0}_{-0.6}) \times 10^{33} T^{-(7.7\pm0.8)}$ cm^3 mol^{-1} s^{-1}, and $k_{rec,\infty}(T) = (1.6^{+1.6}_{-0.5}) \times 10^9 T^{(1.4\pm0.2)}$ cm^3 mol^{-1} s^{-1}, for the temperature dependence of the recombination rate constant in the low- and high-pressure limit, respectively. The corresponding dissociation rate constants, calculated with eq 3, are $k_{diss,0}(T)/[Ar] = (3.0^{+0.3}_{-1.8}) \times 10^{38} T^{-(8.7\pm0.9)} \exp(-4.88 \times 10^3)$ cm^3 mol^{-1} s^{-1} and $k_{diss,\infty}(T) = (4.8^{+4.8}_{-1.5}) \times 10^{14} T^{(0.4\pm0.1)} \exp(-4.88 \times 10^3)$ cm^3 mol^{-1} s^{-1}, respectively.

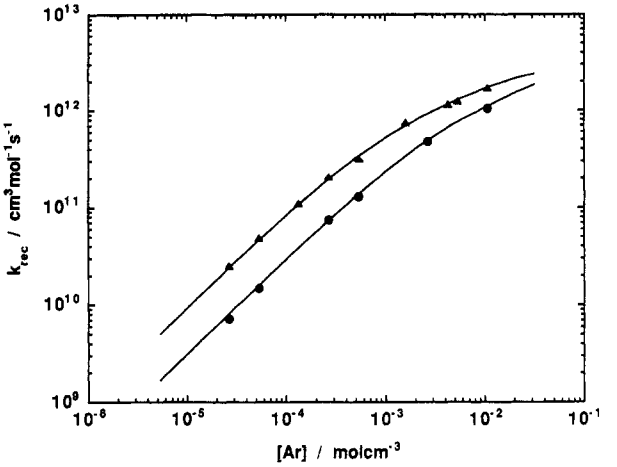

Figure 6. Falloff curves of the reaction NO + NO_2 + Ar → N_2O_3 + Ar at 227 (▲) and 260 K (●).

Conclusion

Kinetic measurements on the N_2O_3 + M = NO_2 + NO + M chemical equilibrium have been carried out by a laser-induced temperature jump method. A small quantity of SiF_4, used as IR sensitizer, is added to equilibrium mixtures involving NO_2, N_2O_3, N_2O_4, and NO, and an excess of argon as third-body gas collider. Following the fast heating of the mixture due to absorption of IR energy by SiF_4, and rapid V–T energy transfer prior to reaction, the recombination rate constant of NO_2 and NO has been determined at 227 and 260 K, and between 0.5 and 200 bar of argon, corresponding to the falloff range. For each total pressure, the recombination rate constant has been examined versus the N_2O_3 concentration, in the presence of an excess of NO and argon as third-body collider. A slight dependence on $[N_2O_3]$ for the low total pressures was observed, and extrapolation of the data to $[N_2O_3] = 0$ leads to the determination of recombination rate constants in conditions where argon is the only effective third body. Experimental data, covering almost 3 decades of pressure, allowed the extrapolation of the recombination rate constants to the high- and low-pressure limits with good confidence. At 227 K, we found $k_{rec,\infty} = (3.5 \pm 1.0) \times 10^{12}$ cm^3 mol^{-1} s^{-1} and $k_{rec,0}/[Ar] = (1.0 \pm 0.5) \times 10^{15}$ cm^3 mol^{-1} s^{-1}, respectively. These experimental results are within a factor of 2 of values obtained using SAC model calculations. The temperature dependences of the recombination rate constants in the high- and low-pressure limit in the range 225–260 K are given by $k_{rec,\infty}(T) = (1.6^{+1.6}_{-0.5}) \times 10^9 T^{(1.4\pm0.2)}$ cm^3 mol^{-1} s^{-1}, and $k_{rec,0}(T)/[Ar] = (1.0^{+1.0}_{-0.6}) \times 10^{33} T^{-(7.7\pm0.8)}$ cm^3 mol^{-1} s^{-1}, respectively. Hence, for the N_2O_3 thermal dissociation reaction, an excellent agreement is found between predicted reaction rate constants calculated using simple statistical models and the values extrapolated from experimental data obtained by the laser-induced temperature jump method. A system such as the dissociation of N_2O_3 into NO_2 and NO, with a relatively low reaction enthalpy of 41.0 kJ/mol, therefore still appears to be well described by statistical theory which implies complete fast intramolecular energy transfer prior to chemical reaction. The kinetics of

isomerization of butadiene and acrolein, which involve still a lower reaction enthalpy, has just been measured in our laboratory and will be reported elsewhere.[35]

Acknowledgment. The authors greatly acknowledge the Swiss National Science Foundation for financial support of this work, and M. Quack, K. Luther and J. Troe for stimulating discussions.

Appendix

Calculation of the High-Pressure Recombination Rate Constant $k_{rec,\infty}$. The nine N_2O_3 vibrational frequencies are, from refs 14 and 15: $\nu_1 = 1832$, $\nu_2 = 1652$, $\nu_3 = 1305$, $\nu_4 = 773$, $\nu_5 = 415$, $\nu_6 = 241$, $\nu_7 = 205$, $\nu_8 = 622$, and $\nu_9 = 70$ cm^{-1}; NO_2 vibrational frequencies, from ref 11: $\nu_1 = 1618$, $\nu_2 = 1320$ and $\nu_3 = 750$ cm^{-1}; NO vibrational frequency, from ref 11: $\nu_1 = 1618$, $\nu_2 = 1320$ and $\nu_3 = 750$ cm^{-1}; NO vibrational frequency, from ref 11: $\nu = 1876$ cm^{-1}. The N_2O_3 rotational constants, from ref 15 are $A = 0.415$, $B = 0.140$, and $C = 0.105$ cm^{-1}; NO_2 rotational constants, from ref 11: $A = 8.001$ cm^{-1}, $B = 0.434$ cm^{-1} and $C = 0.413$ cm^{-1}; NO rotational constants, from ref ref 11: $B = C = 1.696$ cm^{-1}. Reaction coordinate: $\nu_3 = 241$ cm^{-1}. Correlation of the five disappearing oscillations in cm^{-1}: 0.41 (A, N_2O_3) ↔ 0.434 (B, NO_2), 70 (ν_9, N_2O_3) ↔ 0.434 (B, NO_2), 205 (ν_7, N_2O_3) ↔ 1.696 (B, NO), 415 (ν_5, N_2O_3) ↔ 1.696 (B, NO), and 622 (ν_8, N_2O_3) ↔ 8.001 (A, NO_2).

References and Notes

(1) Troe, J. *J. Chem. Phys.* **1977**, *66*, 4745.
(2) Troe, J. *J. Chem. Phys.* **1977**, *66*, 4758.
(3) Troe, J. *J. Chem. Phys.* **1979**, *83*, 114.
(4) Troe, J. *J. Chem. Phys.* **1981**, *75*, 226.
(5) von Puttkamer, K.; Quack, M. *Chimia* **1985**, *39*, 358–360.
(6) Markwalder, B.; Gozel, P.; van den Bergh, H. *J. Chem. Phys.* **1992**, *97*, 5472.
(7) Brunning, J.; Frost, M. J.; Smith, I. W. M. *Int. J. Chem. Kinet.* **1988**, *20*, 957–965.
(8) Carrington, T.; Davidson, N. *J. Phys. Chem.* **1953**, *57*, 418.
(9) Borrell, P.; Cobos, C. J.; Luther, K. *J. Phys. Chem.* **1988**, *92*, 4377–4384.
(10) Bauer, S. H.; Gustavson, M. R. *Discuss. Faraday Soc.* **1954**, *17*, 69.
(11) *JANAF Thermochemical Tables*, 2nd ed.; Stull, D. R.; Prophet, H., Ed.; NSRDS–NBS37: Washington DC, 1971.
(12) Chao, J.; Wilhoit, R. C.; Zwolinski, B. J. *Thermochim. Acta* **1974**, *10*, 359.
(13) Vosper, A. J. *J. Chem. Soc., Dalton Trans.* **1976**, 135.
(14) Bibart, C. H.; Ewing, G. E. *J. Chem. Phys.* **1974**, *61*, 1293.
(15) Chewter, L. A.; Smith, I. W. M.; Yarwood, G. *Mol. Phys.* **1988**, *63*, 843–864.
(16) Smith, I. W. M.; Yarwood, G. *Chem. Phys. Lett.* **1986**, *130*, 24–26.
(17) Smith, I. W. M.; Yarwood, G. *Faraday Discuss. Chem. Soc.* **1987**, *84*, 205–220.
(18) Gozel, P.; Calpini, B.; van den Bergh, H. *Isr. J. Chem.* **1984**, *24*, 210.
(19) Gozel, P. Ph.D. Thesis, EPFL, 1985.
(20) Lynk, E. T.; Major, L. B. *Rev. Sci. Instrum.* **1974**, *45*, 132.
(21) McCarthy, D. E. *Appl. Opt.* **1963**, *2*, 591.
(22) Bass, A. M.; Ledford, Jr. A. E.; Laufer, A. H. *J. Res. Nat. Bur. Stand.* **1976**, *80A*, 143–166.
(23) Vosper, A. J. *J. Chem. Soc. A* **1970**, 625.
(24) Encyclopédie des Gaz; Elsevier: Amsterdam, 1976.
(25) Troe, J. *Ber. Bunsen-Ges. Phys. Chem.* **1983**, *87*, 161.
(26) Gilbert, R. G.; Luther, K.; Troe, J. *Ber. Bunsen-Ges. Phys. Chem.* **1983**, *87*, 169.
(27) Tardy, D. C.; Rabinovitch, B. S. *Chem. Rev.* **1977**, *77*, 369.
(28) Quack, M.; Troe, J. *Gas Kinet. Energy Transfer* **1977**, *2*, 175.
(29) Whitten, G. Z.; Rabinovitch, B. S. *J. Chem. Phys.* **1963**, *38*, 2466.
(30) Quack, M.; Troe, J. *Ber. Bunsen-Ges. Phys. Chem.* **1974**, *78*, 240.
(31) Quack, M.; Troe, J. *Ber. Bunsen-Ges. Phys. Chem.* **1975**, *79*, 170.
(32) Cobos, C. J.; Troe, J. *J. Chem. Phys.* **1985**, *83*, 1010.
(33) Duchovic, R. J.; Hase, W. L.; Schlegel, H. B. *J. Phys. Chem.* **1984**, *88*, 1339.
(34) Peyerimhoff, S.; Lewerenz, M.; Quark, M. *Chem. Phys. Lett.* **1984**, *109*, 563.
(35) Markwalder, B.; Gozel, P.; van den Bergh, H., to be published.